Direct inversion of low-energy electron diffraction (LEED) IV spectra: the surface Patterson function*

2002 J. Phys.: Condens. Matter 14 1231

(http://iopscience.iop.org/0953-8984/14/6/310)

INSTITUTE OF PHYSICS PUBLISHING JOURNAL OF PHYSICS: CONDENSED MATTER

J. Phys.: Condens. Matter **14** (2002) 1231–1236 PII: S0953-8984(02)30448-X

Direct inversion of low-energy electron diffraction (LEED) IV spectra: the surface Patterson function*

S Y Tong[1,2] **and Huasheng Wu**[1]

[1] Department of Physics, The University of Hong Kong, Hong Kong, People's Republic of China
[2] Department of Physics and Materials Science, City University of Hong Kong, Hong Kong, People's Republic of China

Received 2 November 2001, in final form 26 November 2001
Published 1 February 2002
Online at stacks.iop.org/JPhysCM/14/1231

Abstract

We review the symmetrized data acquisition method for producing artifact-free Patterson functions from low-energy electron diffraction (LEED) IV spectra. The differences between LEED Patterson functions and LEED holograms are discussed.

1. Introduction

A Patterson function (PF) [1] gives vector positions of an atom relative to every other atom in the unit cell of a crystal. This information is obtained directly from inversion of diffracted intensities, without the use of an *a priori* model. Low-energy electron diffraction (LEED) PF determination dates back to the work of Adams and Landman [2], who focused on the specular beam. Extension of the method to cover other diffracted beams at normal incidence was carried out by Chang *et al* [3], with very encouraging results. Recently, Wu and Tong [4] applied the method to full beam sets at multiple incidence angles. In the presence of strong multiple scattering, they show that full beam sets at multiple incidence angles are necessary for the recovery of an artifact-free PF. In an artifact-free PF, each high-intensity spot corresponds to a vector position of an atomic pair.

To understand how the PF method works, it is best to write down the diffracted intensities in the far-field approximation [5, 6], due to a collection of scattering centres located at $\vec{r}_1$, $\vec{r}_2$, etc, with respect to an arbitrary origin. Thus, single-scattering and second-order scattering terms are given by

$$I(\vec{k}_i, \vec{k}_f) \propto \left| f_1 e^{-i\vec{q}\cdot\vec{r}_1} + f_2 e^{-i\vec{q}\cdot\vec{r}_2} + f_1 f_3 e^{-i\vec{k}_f\cdot\vec{r}_1} \frac{e^{ikr_{13}}}{r_{13}} e^{i\vec{k}_i\cdot\vec{r}_3} + \cdots \right|^2 \tag{1}$$

where f_i is the scattering factor of atom i. In equation (1), single-scattering events at $\vec{r}_1$ and $\vec{r}_2$, and a second-order event wherein the incident electron first scatters at $\vec{r}_3$, then at $\vec{r}_1$, with

* This article was originally intended to be part of the special issue on holographic and other direct methods for surface structures using electrons and photons which was published as issue 47, volume 13.

$r_{13} = |\vec{r}_1 - \vec{r}_3|$, are explicitly shown. Squaring equation (1) gives the leading cross-term for single-scattering events as

$$I_{1,2}(\vec{k}_i, \vec{k}_f) \propto f_1 f_2^* \mathrm{e}^{-\mathrm{i}\vec{q}\cdot\vec{r}_{12}} \tag{2}$$

where $\vec{r}_{12} = \vec{r}_1 - \vec{r}_2$ and the momentum transfer is $\vec{q} = \vec{k}_f - \vec{k}_i$. To obtain the PF, we multiply the intensity by a phase factor $\mathrm{e}^{\mathrm{i}\vec{q}\cdot\vec{R}}$, which is conjugate to the phase factor of the single-scattering cross-term. It is obvious that at $\vec{R} = \vec{r}_{12}$, the phase factors $\mathrm{e}^{\mathrm{i}\vec{q}\cdot\vec{R}}$ and $\mathrm{e}^{-\mathrm{i}\vec{q}\cdot\vec{r}_{12}}$ cancel at all values of $\vec{q}$. Thus, a sum–integral over an extensive range of $\vec{q}$-values of the form

$$P(\vec{R}) = \left| \sum_{\hat{k}_i} \sum_{\vec{g}_\parallel} \int I(\vec{k}_i, \vec{g}_\parallel + q_\perp \hat{e}_z) \mathrm{e}^{\mathrm{i}\vec{q}\cdot\vec{R}} \, \mathrm{d}q_\perp \right|^2 \tag{3}$$

produces peaks at $\vec{R} = \vec{r}_{ij}$, for all atomic pairs i, j. Here, $P(\vec{R})$ is the PF and $\vec{g}_\parallel$ is a two-dimensional reciprocal-lattice vector (i.e. beam) of the sample. For crystalline materials, only $\vec{r}_{ij}$ within the two-dimensional unit cell provides independent information. The factors $\vec{r}_{ij}$ are three dimensional, pointing between atoms in the same plane as well as in different planes.

It is clear that, in general, multiple-scattering cross-terms from equation (1) such as

$$I_{1,3}(\vec{k}_i, \vec{k}_f) \propto f_1 f_1^* f_3^* \frac{\mathrm{e}^{-\mathrm{i}kr_{13}}}{r_{13}} \mathrm{e}^{\mathrm{i}\vec{k}_i\cdot\vec{r}_{13}} \tag{4}$$

have phase factors $\mathrm{e}^{-\mathrm{i}kr_{13}} \mathrm{e}^{\mathrm{i}\vec{k}_i\cdot\vec{r}_{13}}$. At any $\vec{R}$, these phase factors are not cancelled by $\mathrm{e}^{\mathrm{i}\vec{q}\cdot\vec{R}}$ for more than a subset of $\vec{q}$-values. Therefore, the contributions from multiple-scattering terms can be phase cancelled if many $\vec{q}$-values are used. The exceptions are straight-through multiple-scattering paths. The effects of straight-through multiple-scattering paths, which do not produce artifacts, but shift the positions of spots, are discussed in section 3.

2. The symmetrized data acquisition (SDA) method for LEED Patterson functions

Non-straight-through multiple-scattering events are the main cause of artifacts in LEED PFs. Since a sum over an extensive range of $\vec{q}$-values results in phase cancellation of multiple-scattering terms, such an extensive sum can be obtained if a large set of $\vec{k}_i$-values are used. In LEED, two-dimensional periodicity requires that the diffracted beams have final momenta $\vec{k}_{f\parallel} = \vec{k}_{i\parallel} + \vec{g}_\parallel$. Because a typical LEED screen has a central opening of $\sim 9^\circ$ half-cone angle, the beams are collected within a half-cone angular range of 9°–51°. This incomplete sampling of reciprocal-lattice vectors at a single incidence angle can produce artifacts in the PF [4]. A symmetrized data acquisition (SDA) scheme for processing LEED intensities at multiple incidence angles was introduced recently [4]. In this scheme, the screen opening at one incidence angle is always covered within the Ewald sphere of at least one other incidence angle. The data from symmetry-related incidence angles are included in the sum of equation (3). This step ensures that distances parallel to the surface are accurately determined. The reason will be given in section 3.

3. Accuracy of LEED Patterson functions

The main source of error in LEED PFs comes from the scattering factors. The scattering factor, f_i, causes spots in the PF to shift from $\vec{r}_{ij}$ [5–7]. We shall discuss the accuracy of LEED PFs in comparison with that of LEED holograms. The first difference is that LEED PFs are derived from single-scattering terms while LEED holograms are from second-order terms. Since single scattering is stronger, LEED PFs typically give interatomic distances of many shells of

neighbours while a LEED hologram gives only the nearest one or two neighbours. A second difference is that in LEED PF inversion, the intensities $I(\vec{k}_i, \vec{k}_f)$ are used in the transform of equation (3), and not the normalized functions $\chi(\vec{k}_i, \vec{k}_f) = I(\vec{k}_i, \vec{k}_f)/I_0(\vec{k}_i, \vec{k}_f) - 1$. In LEED holography, $I_0(\vec{k}_i, \vec{k}_f)$ is the scattered intensity at the reference atom. Because $I_0(\vec{k}_i, \vec{k}_f)$ cannot be measured, either in LEED PFs or holograms, its elimination reduces a source of uncertainty. The third difference is that in LEED PFs, the parallel components of the pairwise distances are determined accurately. As mentioned earlier, shifts in the spot positions in either PFs or holograms are caused by scattering factors. Because scattering factors are complex numbers, their dependence on $\vec{k}_i$ or $\vec{k}_f$ introduces shifts in spot positions [5–7]. The SDA scheme completely eliminates this error in the parallel components of LEED PF spots. The reason is simple: for a system with C_2 symmetry, e.g., for each term in the sum of equation (3) that contains a product $f_i(\vec{q}_\parallel) f_j^*(\vec{q}_\parallel)$, there exists another term that contains $f_i(-\vec{q}_\parallel) f_j^*(-\vec{q}_\parallel)$. The shift produced by the former term will be cancelled by an equal but opposite shift from the latter term. Such cancellations are not present in electron holograms, because there, the scattering factor is for angles between $\vec{r}_j$ and $\vec{k}_f$ and not between $\vec{k}_i$ and $\vec{k}_f$. Because dynamical LEED is least accurate in determining atomic positions parallel to the surface, LEED PFs offer a very useful alternative.

For like elements, the phase factors in $f_i f_j^*$ also cancel. Thus, the vertical components of $\vec{r}_{ij}$ are also extremely accurate, if all contributions come from single-scattering events. Unfortunately, higher-order events in which atoms are lined up either in the direction of $\vec{k}_i$ or in that of $\vec{k}_f$ cannot be eliminated. We can see this by considering equation (4). If $\vec{r}_1$ and $\vec{r}_3$ are lined up in the $\vec{k}_f$-direction, then $e^{-ikr_{13}}$ is equivalent to $e^{-ik_f r_1} e^{ik_f r_3}$ and the product $e^{-ikr_{13}} e^{i\vec{k}_i \cdot \vec{r}_{13}}$ is indistinguishable from $e^{-i\vec{q} \cdot \vec{r}_{13}}$. This multiple-scattering cross-term will contribute to the spot at $\vec{R} = \vec{r}_{13}$, like the single-scattering cross-term $f_1 f_3^* e^{-i\vec{q} \cdot \vec{r}_{13}}$. While the phase factors in $f_1 f_3^*$ from the single-scattering cross-term cancel for like elements, the straight-through (i.e. $\vec{r}_1$ and $\vec{r}_3$ lined up in the $\vec{k}_f$-direction) multiple-scattering cross-term has a residual phase factor from the scattering factors.

There are reasons to believe that for many systems, the contributions from these straight-in or straight-out terms may not be too large. First, these terms are for higher-order scattering events and they are decreased by the factor $1/r_{ij}$. Thus, contributions from far neighbours are small. Second, in the set of $\vec{q}$-values, only a subset has near neighbours that are lined up with either $\vec{k}_i$ or $\vec{k}_f$.

The same straight-in or straight-out multiple-scattering terms also contribute to shifts in the spots of LEED holograms [8]. Comparing the vertical shifts in the spot positions of LEED PFs and holograms, the difference is that for the former, the leading term, i.e. single-scattering events, are not shifted for like elements. In LEED holograms, on the other hand, the leading term as well as higher-order straight-in and straight-out terms are all shifted, and by different amounts.

We should mention that the cancellation of parallel component shifts remains valid for any multiple-scattering term, including straight-in or straight-out terms. To summarize: in like-element pairwise distances, the vertical component shifts are caused by straight-in or straight-out higher-order terms. In unlike elements, the vertical component shifts are caused by all orders of scattering events. There is no shift in the parallel components, for like or unlike elements, as long as SDA data are used.

We demonstrate that an artifact-free PF can be obtained by using a wide sampling of wavenumbers k and directions $\vec{k}_i$. The system that we choose for demonstration is Si(111)$\sqrt{3} \times \sqrt{3}$R30°–Ga. By conventional (trial-and-error) dynamical LEED analysis, the surface structure of this system has been determined [9, 10]. A recent dynamical LEED

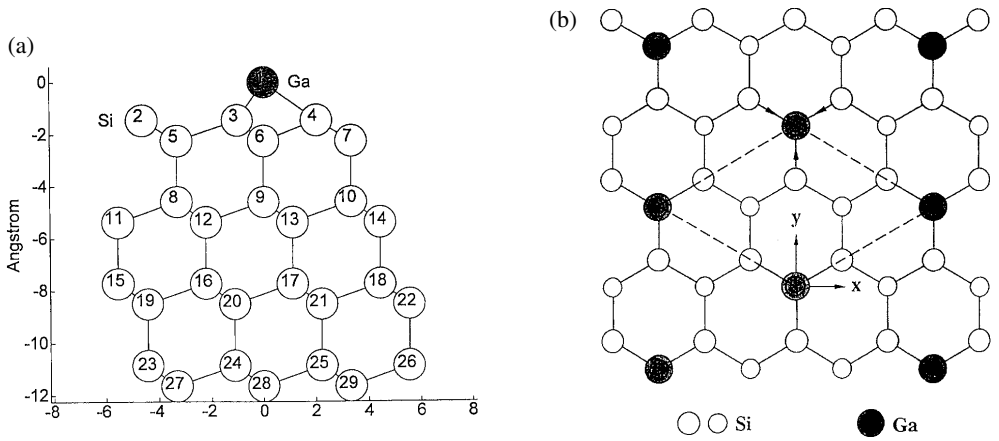

Figure 1. Schematic views of Si(111)$\sqrt{3} \times \sqrt{3}$R30°–Ga with Ga at the T_4 site and 1.46 Å above the topmost Si atoms. (a) The projected side view, and (b) the top view, with $\vec{x}$ along $[0\bar{1}\bar{1}]$ and $\vec{y}$ along $[2\bar{1}\bar{1}]$ directions.

Table 1. Interatomic distances in Å, with the origin at the Ga atom, in the horizontal (x_0-) and vertical (z_0-) directions obtained using atomic positions from the multiple-scattering calculation; and the corresponding quantities (x, z) obtained using spot positions of the PF in figure 3, and their differences (dx, dz). Atomic pairs 1/6 and 6/9 are too close to be resolved and the average value is used for x_0 and z_0; and similarly, for atomic pairs 1/7 and 6/10.

Atomic pairs	x_0	z_0	x	z	dx	dz
1/6, 6/9	0.00	−2.30	0.00	−2.32	0.00	−0.02
1/9	0.00	−4.59	0.00	−4.62	0.00	−0.03
9/28	0.00	−7.04	0.00	−7.00	0.00	0.04
6/7	3.84	0.00	3.84	0.00	0.00	0.00
1/7, 6/10	3.84	−2.30	3.84	−2.30	0.00	0.00
1/10	3.84	−4.59	3.84	−4.50	0.00	0.09
9/29	3.84	−7.04	3.85	−7.00	0.01	0.04
9/12	−2.22	−0.78	−2.23	−0.76	−0.01	0.02
6/12	−2.22	−3.13	−2.23	−3.10	−0.01	0.03
6/16	−2.22	−5.48	−2.22	−5.41	0.00	0.07
1/4	2.02	−1.46	2.02	−1.50	0.00	−0.04
9/21	2.22	−3.91	2.22	−3.90	0.00	0.01
9/25	2.22	−6.26	2.22	−6.20	0.00	0.06

study [10] has obtained an excellent van Hove–Tong R-factor [11] of 0.14, using normal-incidence IV spectra in the 50–400 eV energy range. In figures 1(a) and (b), we show schematic diagrams of the structure of this system, with atoms in the surface region numbered from 1 to 29. We show in figure 2 the sampling of $\vec{k}_f$ using three incidence angles, i.e. $\theta = 0°$; $\theta = 20°$, ϕ along $[11\bar{2}]$; and $\theta = 20°$, ϕ along $[10\bar{1}]$. All values of $\vec{k}_f$ within the dotted circles are sampled. Since the system has a C_3 symmetry,a rotation of 120° is imposed on each set with off-normal incidence. Finally, figure 3 shows the PF obtained from inverting IV spectra calculated by multiple-scattering theory using the incidence directions shown in figure 2. The PF so obtained is completely artifact-free; every spot corresponds to an interatomic vector distance. More significant is the fact that the PF is extremely accurate. Table 1 lists the interatomic distances obtained from the atom positions used in the multiple-

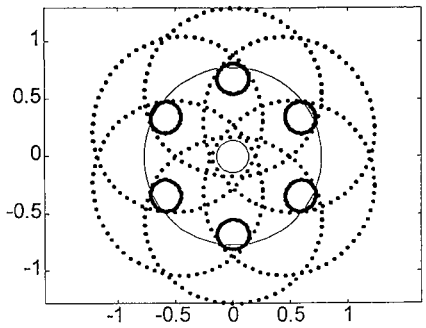

Figure 2. The reciprocal-lattice space $\vec{q}_{11}/k$, using normal and $\theta = 20^\circ$ incidence angles and ϕ along the mirror planes. The small circles represent the central opening of the LEED detector.

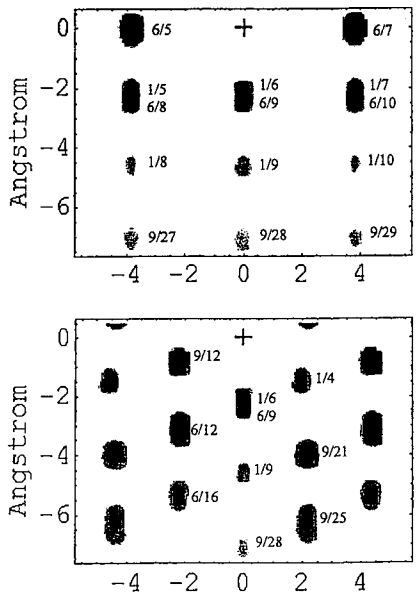

Figure 3. PFs from IV spectra for multiple incidence angles such as those shown in figure 2, obtained using multiple-scattering theory. The upper panel shows the $(2\bar{1}\bar{1})$ plane; the lower panel shows the $(\bar{1}01)$ plane. In each xy-plane, which is parallel to the surface, the lowest 10% of the contours are not shown.

scattering calculation, i.e. x_0 and z_0, and the positions of the spots of the PF of figure 3, i.e. x and z. The average error in the vertical distances is only $\langle|\mathrm{d}z|\rangle = \langle|z - z_0|\rangle = 0.03$ Å, with the largest error being 0.09 Å. The average error in the horizontal distance is even smaller; most spots in the PF occur at exactly the x_0-position, with the largest error being only 0.01 Å.

4. Outlook

LEED is among the most commonly used surface techniques. LEED data collection software is available to measure normal and off-normal IV spectra of multiply diffracted beams over a wide energy range, typically from 50–400 eV, in a matter of a few minutes. It is not

difficult to envisage artifact-free LEED PFs being routinely obtained from unknown systems to study the arrangement of atoms in the first 5–10 system layers. The parallel components are very accurately determined. At the least, the PF method is a powerful 'litmus test' for the correct structure. Once an artifact-free PF is obtained for an unknown system, the interatomic distances determined from the 'best' structure of a trial-and-error method must fit the spots of the PF; otherwise the 'best' structure cannot be correct. The next step is to directly obtain a structural model from the PF. A method for doing this will be published elsewhere [12].

Acknowledgments

We acknowledge helpful discussions with Geng Xu, Simon Ma and Russell Fung. The support of RGC grants HKU7117/98P, HKU7120/00P, HKU7396/00P, DOE grant No DE-FG02-84ER45076 and NSF grant No DMR-9972958 are acknowledged.

References

[1] Patterson A L 1934 *Phys. Rev.* **46** 372
[2] Adams D L and Landman U 1977 *Phys. Rev.* B **15** 3775
[3] Chang C Y, Lin Z C, Chou Y C and Wei C M 1999 *Phys. Rev. Lett.* **83** 2580
[4] Wu Huasheng and Tong S Y 2001 *Phys. Rev. Lett.* **87** 036101
[5] Tong S Y 1999 *Adv. Phys.* **48** 135
[6] Tong S Y, Li H and Huang H 1994 *Surf. Rev. Lett.* **1** 303
[7] Tong S Y, Huang H and Wei C M 1992 *Phys. Rev.* B **46** 2452
[8] Tong S Y 1999 *Surf. Sci.* **433–5** 32
[9] Kawazu A and Sakama H 1988 *Phys. Rev.* B **37** 2704
[10] Chen Wenhua, Wu Huasheng, Ho Wing Kin, Deng B C, Xu Geng and Tong S Y 2000 *Surf. Rev. Lett.* **7** 267–70 and references therein
[11] van Hove M A, Tong S Y and Elconin M H 1977 *Surf. Sci.* **64** 85
[12] Wu Huasheng and Tong S Y, unpublished